Dye-sensitized solar cell based on TiO_2/MnO_2 composite film as working electrode

A Prasetio[1], A M Habieb[1], I Alkian[1], Z Arifin[2] and H Widiyandari[1]

[1] Department of Physics, Diponegoro University, Jl. Prof. Soedharto SH, Semarang, Indonesia.
[2] Department of Mechanical Engineering, Sebelas Maret University, Jl. Ir. Sutami 36A, Surakarta, Indonesia.

E-mail: h.widiyandari@undip.ac.id

Abstract. The purpose of this study is to develop DSSC based on TiO_2/MnO_2 composite film as working electrode. The working electrodes were prepared by the doctor blade method and their characteristics were investigated by using scanning electron microscopy (SEM), X-ray diffraction (XRD) and UV-Vis spectroscopy. Moreover, the performance of DSSCs was performed under simulated AM 1.5G solar illumination using 100 mW/cm^2. The indirect band gap of TiO_2 pure, TiO_2/MnO_2 and TiO_2/MnO_2 6% films are 3.29, 2.98 and 2.81 eV, respectively. The highest power conversion was 0.018 % which corresponds to TiO_2/MnO_2 6% composite film. The results suggest that the MnO_2 added to the semiconductor TiO_2 can improve the efficiency of the DSSCs.

1. Introduction

Energy is the biggest problem will be faced by human due to global energy consumption was growth. The sun is an obvious the largest of clean and sustainable energy source. Photovoltaic (PV) technology, the direct conversion of sunlight to electricity, was classified into three generations of solar cell. The first generation is the silicon wafer based solar cell which categorized into mono-crystalline and poly-crystalline solar cell [1]. The second generation cells are most of thin film solar cells and amorphous (a-Si) solar cell. The third generation cells are the new promising technologies investigated in detail [2]. Dye-sensitized solar cell (DSSC) is one of the third generation PV developed by O'Regan and Grätzel in 1991. The DSSC has attracted attention due to its simple fabrication process, low fabrication cost and promising efficiency in converting energy from solar energy to electricity [3]. Commonly, the DSSC consists of a platinum as counter electrode, an electrolyte containing iodide/ triiodide (I^-/I_3^-), a sensitizer adsorbed on semiconductor surface, and conducting glass usually FTO or ITO coated with nanocrystalline titanium dioxide (TiO_2) semiconductor as working electrode [4]. The working electrode is an important component of the DSSC which its function in injecting the light generated electrons into conduction band of semiconductor and transferring them to the conducting glass [5]. TiO_2 semiconductor has a key role as working electrode due to its high transparency for visible light, chemically stable, non-toxic, and controllable electric properties. However, TiO_2 has a relatively high energy gap (Eg=3.2 eV for anatase) and works at a small fraction of the solar spectrums (ultra-violet region) [6-8]. The further development in terms of both mechanisms DSSC fabrication and material synthesis are needed to

improve the power efficiency. One promising approach is based on adding other semiconductor materials with lower energy gap into TiO_2 semiconductor. Pure manganese oxide (MnO_2) semiconductor has direct energy gap of about 2.5 eV which can decrease the energy gap of TiO_2 and increase the power efficiency of DSSC [9-11]. Thus, the main purpose of this research is to improve performance of the DSSC through band gap engineering on working electrode by adding MnO_2 to TiO_2.

In this paper, TiO_2/MnO_2 composite films were synthesized and deposited onto FTO glass substrates using the doctor blade method. The characteristics of TiO_2/MnO_2 composite films were characterized by using scanning electron microscopy (SEM), energy dispersive microanalysis (EDS), X-ray diffraction (XRD) and ultraviolet-visible (UV-Vis) spectroscopy. The performance of the DSSCs was measured under AM 1.5G solar illumination at 100 mW/cm^2 light intensity.

2. Method

2.1. Materials

TiO_2 P25 degusa powder (Sigma Aldrich, USA) was used as working electrode layer. $KMnO_4$ powder (Merck, Germany) was used as precursor of MnO_2 powder. Platinum paste (Dyesol, Australia) was used as counter electrode layer. Fluorine-doped tin oxide (FTO) glass substrate (15Ω/sq, 2.3 mm thickness, Dyesol, Australia) was used as conducting glass. Electrolyte HSE containing iodide and triiodide (Dyesol, Australia) solution was used as the transport for redox mediator between two electrodes. Ruthenium dye N719 (Dyesol, Australia) was used as sensitizer and sunlight harvester. Sealant (Dyesol, Australia) was used for sealing spacer DSSC device for longer term application.

2.2. MnO_2 powder synthesis

To synthesis MnO_2 powder, 0.75 gr $KMnO_4$ was solved in 20 ml aqua DM and 10 ml ethanol (Merck, Germany) and stirred for 15 min at room temperature. The $KMnO_4$ solution was filtered by using filter paper for 24 h. The solution precipitate into blackish MnO_2 sediment as a result of chemical reaction. The MnO_2 sediment was dried at 90°C for 5 h and milled for 15 min.

2.3. Preparation of the working electrodes

The FTO glass substrate with area 2.5 x 2.5 cm^2 was washed with ethanol and aquades several times. The MnO_2 powder was added into TiO_2 powder and milled for 15 min in high energy milling 3D (Nanotech Indonesia, Indonesia). This process was enough to provide homogeneous powder. The TiO_2 P25 powder with various concentrations of 0, 2 and 6% of the MnO_2 powder were named as TiO_2 pure, TiO_2/MnO_2 2% and TiO_2/MnO_2 6%, respectively.

To prepare TiO_2/MnO_2 paste, the mixture of TiO_2/MnO_2 powder (MnO_2 content: 0, 2 and 6%) was dispersed into the binder which prepared from our previous research [12]. TiO_2/MnO_2 paste was deposited onto the FTO glass substrate by using the doctor blade method with thickness of about 5 μm and active area 1 x 1 cm^2. After that, the working electrode was sintered at 500°C for 45 min then immersed into a 0.3 mM ruthenium dye N719 in a mixture of tert-butanol and acetonitrile solution for 24 h at room temperature.

2.4. Preparation of the Pt-counter electrode

To prepare the counter electrode, two holes (1 mm diameter on active surface) were drilled through for each FTO glass substrate by using diamond bor. The FTO glass substrate was washed with ethanol and aquades. Platinum paste was deposited onto the FTO glass substrate by using the doctor blade method with thickness is equal to the thickness of the scotch tape with active area 1 x 1 cm^2. After drying at 80°C, the Pt-counter electrode was sintered at 450°C for 60 min.

2.5. Assembly of the DSSC

The working electrode was assembled into a sandwich like structure with the Pt-counter electrode (Figure 1). The sealant was put on as sealing spacer between two electrodes, the inner dimensions 1.5 mm wider than TiO_2/MnO_2 layer. The working electrode and the Pt-counter electrode assembled were secured using a binder clip on each side. The electrolyte solution was injected through one of the holes. Finally, the holes were sealed with silicon glue to prevent evaporation.

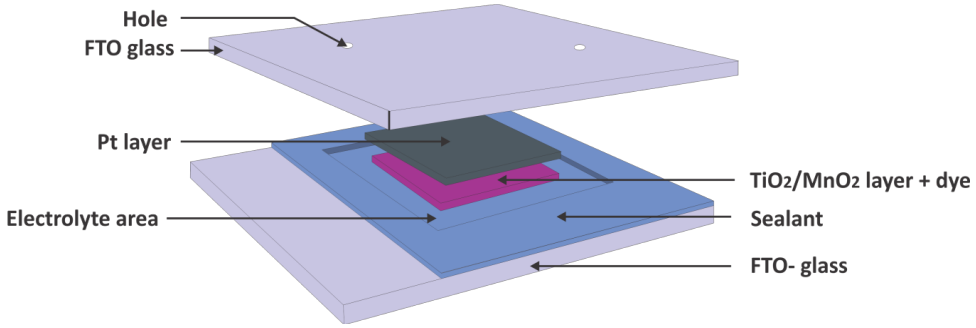

Figure 1. A sandwich like structure for DSSC.

2.6. Chacterization and measurement

The structural analysis of the TiO_2/MnO_2 films was characterized using XRD (Rigaku-Denki Corp, Japan) with a CuKα source (λ= 0.154 nm). The surface morphology and elemental composition of the TiO_2/MnO_2 films were observed using SEM-EDS (JEOL JSM-6360 LA, Japan). The optical properties of the TiO_2/MnO_2 films were obtained using Shimadzu 1240 SA UV-Vis spectroscopy (Shimadzhu, Japan). The photovoltaic performance of the DSSCs was measured using a Keithley 2602A sourcemeter (Keithley Instrument, USA) under AM 1.5G solar illumination at 100 mW/cm^2 light intensity.

3. Results and discussion

High-magnification of SEM images of the TiO_2/MnO_2 samples are shown in Figure 2. By comparing particles with the scale bar, we determined that the average diameter of the TiO_2 particles was approximately 200 nm. Large particle sizes could be attributed to a strong light scattering and less dye adsorption leading to lower efficiency of the DSSCs. These are should be caused by small surface area of the samples. In other hand, both MnO_2 and TiO_2 particles have a similar shape as shown in Figure (b) and (c).

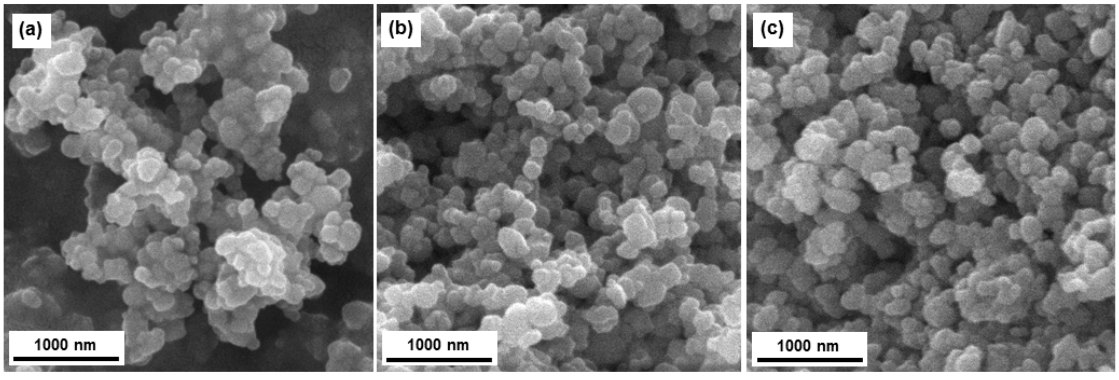

Figure 2. High-magnification SEM images of the(a) TiO_2 pure; (b) TiO_2/MnO_2 2% and (c) TiO_2/MnO_2 6% samples.

Figure 3 shows chemical composition of the samples which obtained using EDS. Peaks at 0.525, 4.508 and 5.894 keV agree with O, Ti and Mn, respectively. It proves that the samples consisted of only three elements.

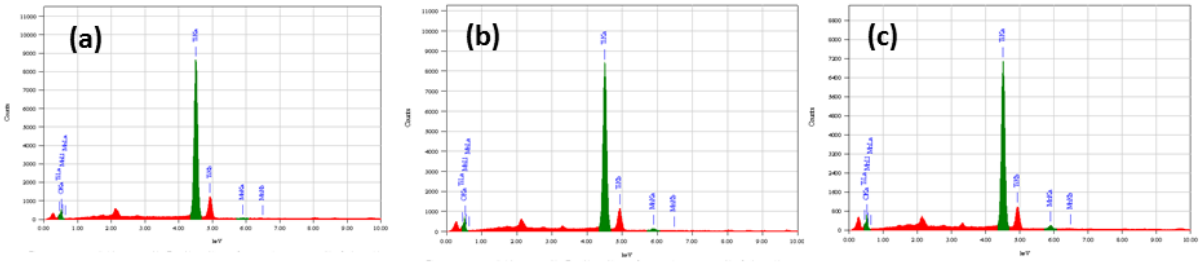

Figure 3. EDS observation of the (a) TiO_2 pure; (b) TiO_2/MnO_2 2% and (c) TiO_2/MnO_2 6% samples.

The XRD patterns for TiO_2, TiO_2/MnO_2 2% and TiO_2/MnO_2 6% samples are shown in Figure 4(a). Similar patterns were obtained from the samples. The XRD patterns agree with the Joint Committee on Powder Diffraction Standards (JCPDS) database no. 21-1272. The strongest peaks at 25.4, 37.8 and 48.0° correspond respectively to the (101), (004) and (200) planes of anatase phase. Figure 4(b) shows that d-spacing of (101) lattice plane of TiO_2 decreases should be caused by increasing of MnO_2 content. However, MnO_2 patterns are not shown clearly in the XRD patterns.

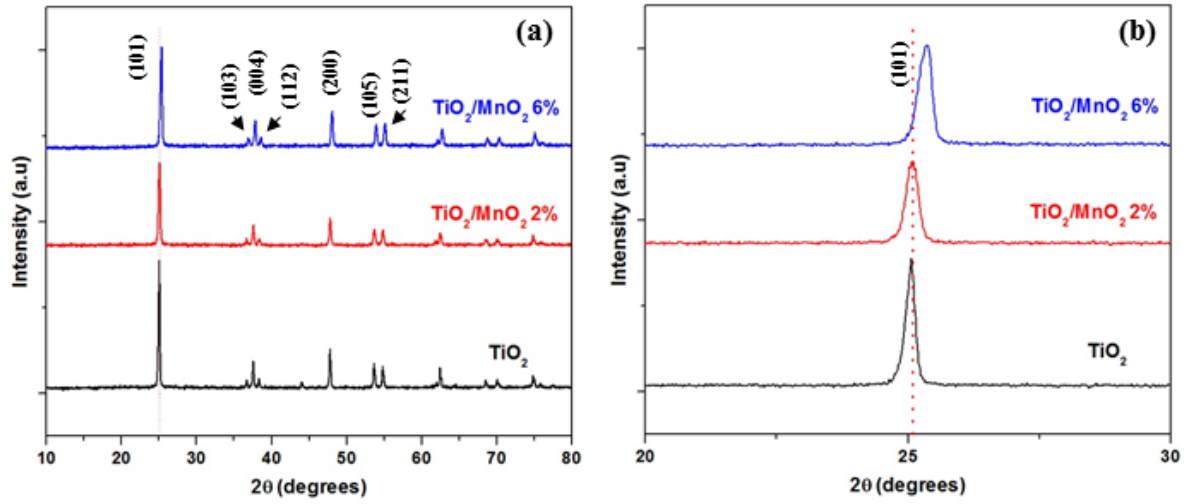

Figure 4. (a) The XRD patterns of the TiO_2, TiO_2/MnO_2 2% and TiO_2/MnO_2 6% and (b) details of the XRD patterns around from 25° to 30° 2θ values.

The optical energy gap of each sample can be calculated and estimated by using Tauc's plot and equation (1):

$$(\alpha h\nu) = A(h\nu - E_g)^n \quad (1)$$

where α is the optical absorption coeffcient, $h\nu$ is photon energy, A is the constant, E_g is optical energy gap and the exponent n is depending on the nature of the transition (n = 2 corresponds to indirect energy gap of anatase TiO_2) [13]. Therefore, the plot of $(\alpha h\nu)^{1/2}$ vs $h\nu$ represent E_g, as shown in Figure 5.

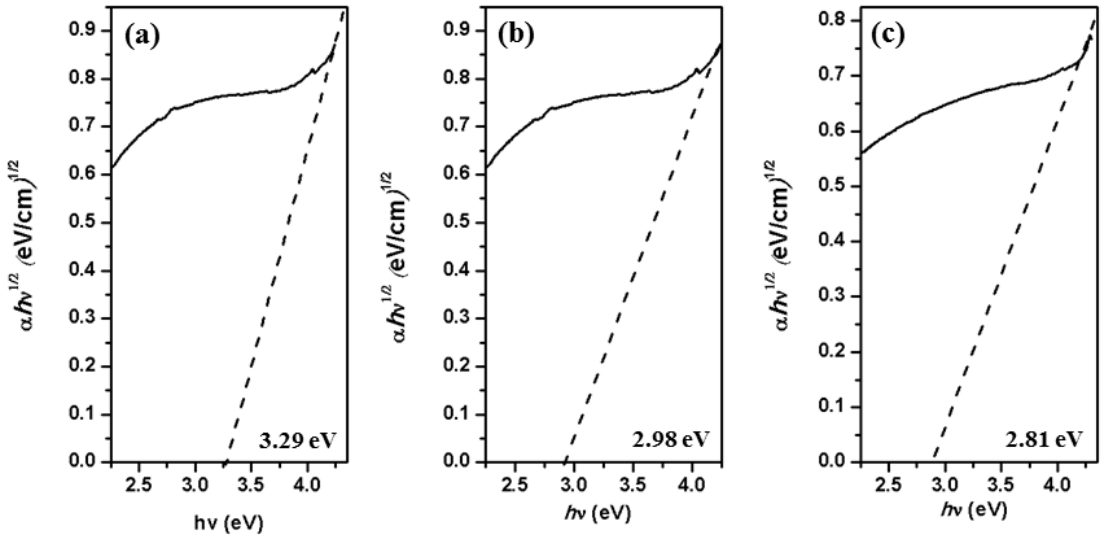

Figure 5. *Plot* $(\alpha h\nu)^{1/2}$ vs $h\nu$ of (a) TiO_2, (b) TiO_2/MnO_2 2% and (c) TiO_2/MnO_2 6% samples.

The energy gap of TiO_2, TiO_2/MnO_2 2% and TiO_2/MnO_2 6% films of approximately 3.29, 2.98 and 2.81 eV, respectively. The energy gap of various films is found decrease along with increases of MnO_2 concentration. Lower energy gap to be responsible to enhancement of electron injection and transport [14].

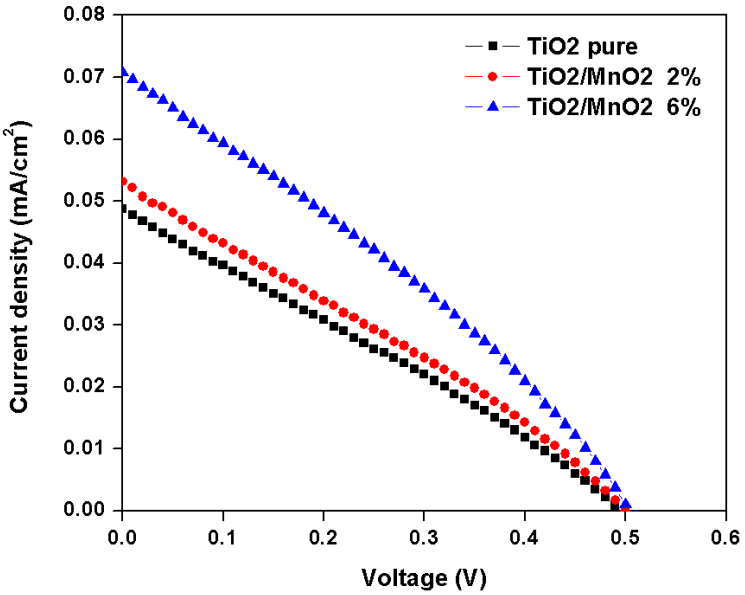

Figure 6. J-V curves of DSSCs for TiO_2, TiO_2/MnO_2 2% and TiO_2/MnO_2 6%.

Figure 6 shows the current density-voltage (J-V) curve of the DSSCs with various concentrations of the MnO_2 which were performed under simulated AM 1.5G solar illumination using 100 mW/cm^2. The conversion efficiency (η) of the DSSCs is determined by short-circuit current density (J_{sc}), open-circuit potential (V_{oc}) and the intensity of the incident light per unit area (P_{in}). The overall conversion efficiency is shown in equation (2).

$$\eta = \frac{J_{sc} \cdot V_{oc} \cdot FF}{P_{in}} \times 100\% \quad (2)$$

The fill factor (FF) can be calculated according to the equation (3) below:

$$FF = \frac{J_{\max} \cdot V_{\max}}{J_{sc} \cdot V_{oc}} \quad (3)$$

where J_{max} and V_{max} are the current density and potential at the point of the maximum power respectively [15]. The photovoltaic performance of DSSCs based on TiO_2/MnO_2 electrodes with different MnO_2 contents are listed in Table 1.

Table 1. Photovoltaic properties of DSSCs with various working electrodes

Photoanode	J_{sc} (mA.cm^{-2})	V_{oc} (V)	Fill Factor	Efficiency (%)
TiO_2	0.0487	0.4948	0.2773	0.0067
TiO_2/MnO_2 2%	0.0531	0.4997	0.2811	0.0075
TiO_2/MnO_2 6%	0.0707	0.5049	0.3008	0.0108

Both the curve and the table show that the DSSC with TiO_2/MnO_2 6% photoanode has the highest value of J_{sc} as well as efficiency. Meanwhile, the DSSC with TiO_2 pure photoanode has the lowest value of J_{sc} as well as efficiency. The results show that the MnO_2 added to the TiO_2 semiconductor can improve both the efficiency and J_{sc} of the DSSCs.

4. Conclusion

The DSSCs using TiO_2/MnO_2 films as working electrode have been successfully fabricated by using the doctor blade method. By adding of MnO_2 to TiO_2 semiconductor can decrease energy gap of the TiO_2, which means the DSSCs can work under visible light and harvest energy optimally. Additionally, lower energy gap responsibles to enhance injection as well as transport of electron. The enhancement of electron injection and transport leads to the improvement of J_{sc}. Consequently, FF and efficiency of the DSSC increases significant enough.

Acknowledgement

Financial support from Ministry of Research, Technology and Higher Education of Indonesia is gratefully acknowledged. In addition, we would thank to La Ode Yusni Malik for valuable discussion.

References

[1] Barham K W J, Mazzer M and Clive B 2006 *Nat. Mater.* **5** 161
[2] Sharma S, Jain K K and Sharma A 2015 *Mater. Sci. Appl.* **6** 1145
[3] O'Regan B and Grätzel M 1991 *Nature* **353** 737
[4] Nazeeruddin Md K, Baranoff E and Grätzel M 2011 *Solar Energy* **85** 1172
[5] Grätzel M 2003 *J. Photochem. Photobio. C: Photochem. Rev.* **4** 145
[6] Sedghi A and Miankushki H N 2012 *Int. J. Elecrochem. Sci.* **7** 12078
[7] Qin W, Lu S, Wu X and Wang S 2013 *Int. J. Elecrochem. Sci.* **8** 7984
[8] Lin Y, Jiang Z, Zhu C, Hu X, Zhang X, Zhu H, Fan J and Lin S H 2013 *J. Mater. Chem.* A **1** 4516
[9] Li T, Wu J, Xiao X, Zhang B, Hu Z, Zhou J, Yang P, Chen X, Wang B and Huang L 2016 *RSC Adv.* **6** 13914
[10] Toufiq A M, Wang F, Javed Q, Li Q and Li Y 2014 *Appl. Phys.* A **116** 1127

[11] Brus V V, Pidkamin L J, Abashin S L, Kovalyuk Z D, Marynchuk P D and Chugai O M 2012 *Optic. Mater.* **34** 1940
[12] Prasetio A, Purwanto A, Subagio A and Widiyandari H 2016 *6th AIP Conf. Proc. Nanosci. Nanotech. Symp. 2015(Surakarta)* vol 1710 (College Park: Maryland/AIP Publishing) 030054
[13] Buchholz D B, Liu J, Marks T J, Zhang M and Chang R P H 2009 *ACS Appl. Mater. Interfaces* **1** 2147
[14] Sua H, Huanga Y T, Changa Y H, Zhaia P, Haua N Y, Cheunga P C H, Yehc W T, Weid T C and Fenga S P 2015 *Electrochimica Acta* **182** 230
[15] Nazeeruddin M K, Kay A, Rodicio I, Humphry-Baker R, Muller E, Liska P, Vlachopoulos N and Gratzel M 1993 *J. Am. Chem. Soc.***115** 6382